1-1-2015

Low voltage polymer network liquid crystal for infrared spatial light modulators

Fenglin Peng
University of Central Florida

Daming Xu
University of Central Florida

Haiwei Chen
University of Central Florida

Shin-Tson Wu
University of Central Florida

Low voltage polymer network liquid crystal for infrared spatial light modulators

Fenglin Peng, Daming Xu, Haiwei Chen, and Shin-Tson Wu*

CREOL, The College of Optics and Photonics, University of Central Florida, Orlando, Florida 32816, USA
*swu@ucf.edu

Abstract: We report a low-voltage and fast-response polymer network liquid crystal (PNLC) infrared phase modulator. To optimize device performance, we propose a physical model to understand the curing temperature effect on average domain size. Good agreement between model and experiment is obtained. By optimizing the UV curing temperature and employing a large dielectric anisotropy LC host, we have lowered the 2π phase change voltage to 22.8V at 1.55μm wavelength while keeping response time at about 1 ms. Widespread application of such a PNLC integrated into a high resolution liquid-crystal-on-silicon (LCoS) for infrared spatial light modulator is foreseeable.

OCIS codes: (230.3720) Liquid-crystal devices; (120.5060) Phase modulation; (160.3710) Liquid crystals.

References and links

1. U. Efron, *Spatial Light Modulator Technology: Materials, Devices, and Applications* (Marcel Dekker, 1994).
2. S. Quirin, D. S. Peterka, and R. Yuste, "Instantaneous three-dimensional sensing using spatial light modulator illumination with extended depth of field imaging," Opt. Express **21**(13), 16007–16021 (2013).
3. H. Ren and S.-T. Wu, *Introduction to Adaptive Lenses* (Wiley, 2012).
4. F. Feng, I. H. White, and T. D. Wilkinson, "Free space communications with beam steering a two-electrode tapered laser diode using liquid-crystal SLM," J. Lightwave Technol. **31**(12), 2001–2007 (2013).
5. F. Peng, Y. Chen, S.-T. Wu, S. Tripathi, and R. J. Twieg, "Low loss liquid crystals for infrared applications," Liq. Cryst. **41**(11), 1545–1552 (2014).
6. R. A. Forber, A. Au, U. Efron, K. Sayyah, S. T. Wu, and G. C. Goldsmith II, "Dynamic IR scene projection using the Hughes liquid crystal light valve," Proc. SPIE **1665**, 259–273 (1992).
7. F. Peng, H. Chen, S. Tripathi, R. J. Twieg, and S.-T. Wu, "Fast-response infrared phase modulator based on polymer network liquid crystal," Opt. Mater. Express **5**(2), 265–273 (2015).
8. B. M. Moslehi, K. K. Chau, and J. W. Goodman, "Optical amplifiers and liquid-crystal shutters applied to electrically reconfigurable fiber optic signal processors," Opt. Eng. **32**(5), 974–981 (1993).
9. G. Zhu, B. Y. Wei, L. Y. Shi, X. W. Lin, W. Hu, Z. D. Huang, and Y. Q. Lu, "A fast response variable optical attenuator based on blue phase liquid crystal," Opt. Express **21**(5), 5332–5337 (2013).
10. J. Sun, S.-T. Wu, and Y. Haseba, "A low voltage submillisecond-response polymer network liquid crystal spatial light modulator," Appl. Phys. Lett. **104**(2), 023305 (2014).
11. S.-T. Wu, "Birefringence dispersions of liquid crystals," Phys. Rev. A **33**(2), 1270–1274 (1986).
12. J. Sun and S. T. Wu, "Recent advances in polymer network liquid crystal spatial light modulators," J. Polym. Sci., Part B, Polym. Phys. **52**(3), 183–192 (2014).
13. J. Yan, Y. Chen, S.-T. Wu, S.-H. Liu, K.-L. Cheng, and J.-W. Shiu, "Dynamic response of a polymer-stabilized blue-phase liquid crystal," J. Appl. Phys. **111**(6), 063103 (2012).
14. I. Dierking, "Polymer network–stabilized liquid crystals," Adv. Mater. **12**(3), 167–181 (2000).
15. D. Xu, J. Yan, J. Yuan, F. Peng, Y. Chen, and S.-T. Wu, "Electro-optic response of polymer-stabilized blue phase liquid crystals," Appl. Phys. Lett. **105**(1), 011119 (2014).
16. Y.-H. Fan, Y.-H. Lin, H. Ren, S. Gauza, and S.-T. Wu, "Fast-response and scattering-free polymer network liquid crystals for infrared light modulators," Appl. Phys. Lett. **84**(8), 1233–1235 (2004).
17. S. A. Serati, X. Xia, O. Mughal, and A. Linnenberger, "High-resolution phase-only spatial light modulators with submillisecond response," Proc. SPIE **5106**, 138–145 (2003).
18. J. Sun, Y. Chen, and S.-T. Wu, "Submillisecond-response and scattering-free infrared liquid crystal phase modulators," Opt. Express **20**(18), 20124–20129 (2012).
19. F. Du and S.-T. Wu, "Curing temperature effects on liquid crystal gels," Appl. Phys. Lett. **83**(7), 1310–1312 (2003).

#226549 - $15.00 USD Received 7 Nov 2014; revised 14 Jan 2015; accepted 15 Jan 2015; published 28 Jan 2015

20. F. Du, S. Gauza, and S.-T. Wu, "Influence of curing temperature and high birefringence on the properties of polymerstabilized liquid crystals," Opt. Express **11**(22), 2891–2896 (2003).
21. D.-K. Yang, Y. Cui, H. Nemati, X. Zhou, and A. Moheghi, "Modeling aligning effect of polymer network in polymer stabilized nematic liquid crystals," J. Appl. Phys. **114**(24), 243515 (2013).
22. S.-T. Wu and C.-S. Wu, "Experimental confirmation of the Osipov-Terentjev theory on the viscosity of nematic liquid crystals," Phys. Rev. A **42**(4), 2219–2227 (1990).
23. H. Kneppe, F. Schneider, and N. K. Sharma, "Rotational viscosity γ1 of nematic liquid crystals," J. Chem. Phys. **77**(6), 3203–3208 (1982).
24. H. Chen, F. Peng, Z. Luo, D. Xu, S.-T. Wu, M.-C. Li, S.-L. Lee, and W.-C. Tsai, "High performance liquid crystal displays with a low dielectric constant material," Opt. Mater. Express **4**(11), 2262–2273 (2014).
25. S.-T. Wu, A. M. Lackner, and U. Efron, "Optimal operation temperature of liquid crystal modulators," Appl. Opt. **26**(16), 3441–3445 (1987).
26. J. Yan, Y. Chen, S.-T. Wu, and X. Song, "Figure of merit of polymer-stabilized blue phase liquid crystals," J. Disp. Technol. **9**(1), 24–29 (2013).

1. Introduction

Liquid crystal (LC) spatial light modulators (SLMs) [1] have been widely used in adaptive optics [2], adaptive lens [3], laser beam control [4–7] and fiber-optic communication [8, 9]. Low operation voltage for 2π phase change ($V_{2\pi}$) and fast response time are critical requirements for these applications. Most SLMs using a nematic LC has advantage in low $V_{2\pi}$, however, its response time is relatively slow (50-100 ms). Polymer network liquid crystal (PNLC) is a promising candidate for SLM because of its simple fabrication method, sub-millisecond response time, and large phase change (δ) which is governed by:

$$\delta = 2\pi d\Delta n / \lambda, \tag{1}$$

where d is the cell gap, Δn is the LC birefringence, and λ is the operation wavelength. Two major technical challenges of PNLC are: 1) its $V_{2\pi}$ is relatively high, originating from strong anchoring force exerted from submicron polymer network domain sizes, and 2) light scattering. Recently, Sun et al [10] demonstrated a PNLC with $V_{2\pi}$ = 23V at λ = 514nm with a significantly suppressed light scattering (~3%). Although a 3% scattering seems low, when several devices are cascaded together the total optical loss is still significant.

As the wavelength increases, the LC birefringence gradually decreases and then saturates in the infrared (IR) region [11]. As a result, the available phase change decreases. From Sun's multi-layer model, the on-state voltage of a PNLC device is proportional to the cell gap as [10]:

$$V_{on} \propto \frac{\pi d}{d_1}\sqrt{\frac{K_{11}}{\varepsilon_0\Delta\varepsilon}}, \tag{2}$$

here d_1 is the average domain size, K_{11} is the splay elastic constant, ε_0 is the electric permittivity and $\Delta\varepsilon$ is the dielectric anisotropy. Therefore, for a given domain size and LC material, $V_{2\pi}$ increases as the cell gap or wavelength increases. Unlike a nematic liquid crystal, the LC molecules in a PNLC device are partitioned into numerous submicron domains. The restoring force on the deformed LC directors is dominated by the anchoring force of polymer network [12]. However, the anchoring force is not uniform over the LC medium [13]. The LC molecules closer to polymer network would experience a stronger anchoring force than those in the center. Therefore, they will rotate by different angles when an electric field is applied. Moreover, stronger anchoring force helps restore the LC molecules with faster response time. Therefore when the applied voltage is high enough, the LC molecules with weaker anchoring force will be reoriented to a larger angle and it takes longer time to restore back. As a result, multiple decay processes take place [14, 15] and response time increases. Fan et al [16] have demonstrated a PNLC light modulator at λ = 1.55μm with $V_{2\pi}$≈60V in a reflective mode. However, the spatial phase profile is not uniform due to employing a non-mesogenic monomer (M1) [12]. On the other hand, the commonly

#226549 - $15.00 USD Received 7 Nov 2014; revised 14 Jan 2015; accepted 15 Jan 2015; published 28 Jan 2015

used high resolution liquid-crystal-on-silicon (LCoS) has a maximum voltage of 24V [17]. Therefore, to integrate infrared PNLC with LCoS for widespread applications, there is a need to develop a PNLC with $V_{2\pi}$<24V, while keeping fast response time and spatially uniform phase profile.

In this paper, we demonstrate a reflective-mode PNLC phase modulator with $V_{2\pi}$ = 22.6V at λ = 1.55μm and response time τ≈1.13ms. To achieve such a low operation voltage while keeping fast response time in the IR region, we optimized UV curing condition and LC host. First, we investigated the curing temperature effects on domain size, which plays a critical role affecting the operation voltage and response time. A physical model was proposed to describe this correlation. Excellent agreement between model and experiment is obtained. Besides, the performance of a PNLC is heavily affected by the properties of the LC host. Therefore, we define a figure of merit (*FoM*), which is independent of device structure and domain size, for comparing the LC hosts. The temperature effect on *FoM* was also studied. For a given LC host, there is an optimal operation temperature for a PNLC, where *FoM* has a maximum value.

2. Sample preparation

To fabricate PNLCs, we prepared a precursor by mixing 92.5wt% of LC host (JC-BP07N, JNC), with 7.0 wt% of monomer (RM257, Merck) and 0.5 wt% of photo-initiator (BAPO, Genocure). Here, we used RM257 (a LC monomer) to maintain good alignment and obtain uniform phase profile. We filled the precursor into homogeneous LC cells (indium tin oxide glass substrates). The cell gap was controlled at ~11.8μm. The clearing point (T_c) of JC-BP07N is 87°C. If the curing temperature is close or higher than T_c, then the LC molecules will not align well with the rubbing directions, resulting in severe light scattering after polymerization. Thus, during UV curing process we controlled the curing temperature for each cell from 0°C to 70°C separately. Here, a UV light-emitting diode (LED) lamp (λ = 385nm, Intensity is 300 mW/cm^2) was employed and the exposure time was one hour.

3. Curing temperature effect

To characterize the electro-optic properties of each PNLC cell, we measured its voltage-dependent transmittance (VT) with a laser beam at λ = 1.55μm. The PNLC cells were sandwiched between two crossed polarizers, with the rubbing direction at 45° to the polarizer's transmission axis. The phase change of reflective mode is twice of transmissive mode due to the doubled optical path.

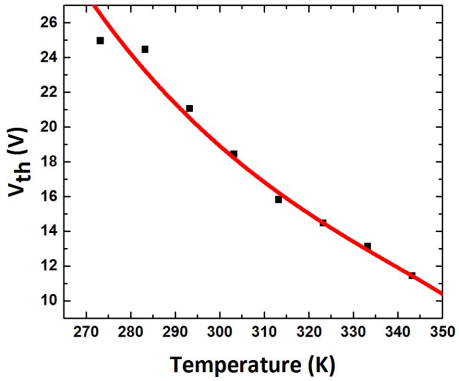

Fig. 1. Curing temperature dependent threshold voltage of PNLCs: dots stand for measured data and red line for fitting curve with Eq. (9).

Figure 1 depicts the measured threshold voltage (V_{th}) of PNLCs cured at different temperatures. As the curing temperature increases from 0°C to 70°C, V_{th} decreases from

#226549 - $15.00 USD Received 7 Nov 2014; revised 14 Jan 2015; accepted 15 Jan 2015; published 28 Jan 2015

25.0V to 10.9V. This is because the LC viscosity decreases exponentially with increased curing temperature, which accelerates the polymer diffusion rate. Thus, the domain size is inversely proportional to the LC viscosity [18]. Therefore, higher curing temperature produces coarser polymer network [19, 20] and generates PNLC with larger average domain size. The anchoring force provided by polymer network becomes weaker with a larger domain size and coarser polymer network, and thus the driving voltage decreases [21].

Du et al [19, 20] explored the curing temperature effects on LC gels, but no quantitative model was developed to correlate the curing temperature with domain size. Based on the multi-layer model, free relaxation time (τ) is insensitive to the cell gap and it is governed by the average domain size (d_1) as:

$$\tau = \gamma_1 d_1^2 / (K_{11}\pi^2), \tag{3}$$

where γ_1 is the rotational viscosity, K_{11} is the splay elastic constant and d_1 is the average domain size. Therefore, the average domain size at each curing temperature can be obtained by measuring the free relaxation time of the PNLC. To measure the free relaxation time, we applied a small bias voltage to each PNLC sample to get a small initial phase change δ_0 in order to satisfy the small angle approximation [22]. At t = 0, the voltage was removed instantaneously and optical signal recorded by a photodiode detector. The time dependent phase relaxation curve can be expressed as:

$$\delta(t) = \delta_0 \exp(-2t/\tau). \tag{4}$$

By fitting with Eq. (4), the free relaxation time for each PNLC sample can be extracted. Next, we calculated the average domain size based on Eq. (3).

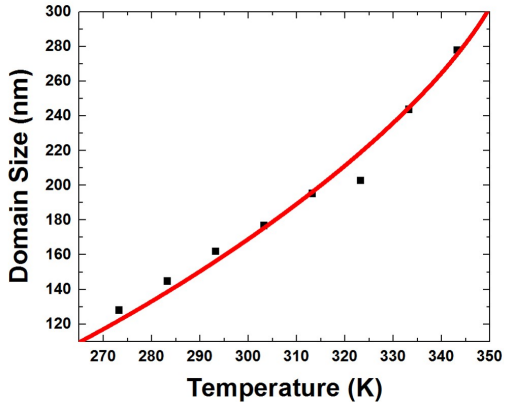

Fig. 2. Curing temperature dependent average domain size of PNLCs: dots stand for the measured data and red line for fitting curve with Eq. (8).

Figure 2 depicts the domain size obtained at each curing temperature. As the curing temperature increases from 0°C to 70°C, the average domain size increases from 130nm to 280nm because of the increased monomer diffusion rate. The increased domain size has pros and cons. On the positive side, it weakens the anchoring force, leading to a lower operation voltage. But on the negative side, the response time increases. From Fig. 2, even the curing temperature reaches 70°C the domain size is only 280nm, which is still much smaller than the infrared wavelength (λ = 1.55μm). Thus, light scattering remains negligible. Based on Stokes-Einstein theory, the domain size is inversely proportional to the viscosity [18]. Thus, the domain size (d_1) can be expressed as:

$$d_1^2 \sim \frac{k_B T t}{3\pi\eta R}, \tag{5}$$

#226549 - $15.00 USD Received 7 Nov 2014; revised 14 Jan 2015; accepted 15 Jan 2015; published 28 Jan 2015

here k_B is the Boltzmann constant, T is the Kelvin temperature, η is the flow viscosity, R is the radius of the particles, and t is the time interval. Among these parameters, R and t are independent of temperature. The flow viscosity is much smaller than rotational viscosity but has similar temperature dependence [23, 24]:

$$\eta \sim S \cdot \exp(E_b / k_B T), \tag{6}$$

$$S = (1 - \mathrm{T}/\mathrm{T_c})^{\beta}, \tag{7}$$

here S is the order parameter, E_b is the fitting parameter related to activation energy, T_c is the clearing point, and β is a material constant. By substituting Eq. (6) into Eq. (5), the curing temperature dependent domain size can be expressed as:

$$d_1 = A \cdot \sqrt{\frac{T \exp(-\mathrm{E_b}/\mathrm{k_B T})}{(1 - T/T_c)^{\beta}}}, \tag{8}$$

where A is a fitting parameter. We fitted average domain size d_1 at various curing temperatures with Eq. (8). Good agreement is obtained as shown in Fig. 2. The fitting parameters are A = 106.9 $nm/\sqrt{K}$ and E_b = 131.3 meV. The material constant β = 0.16 is obtained independently by fitting the temperature dependent birefringence data. The melting point of JC-BP07N is T_c = 87°C. The adjustable parameter A is governed by the viscosity of LC host, monomer concentration, and UV dosage. A LC with higher rotational viscosity contributes to smaller domain size [18]. In the meantime, higher monomer concentration and UV dosage contribute to a smaller average domain size [14]. Besides, the threshold voltage (V_{th}) is inversely proportional to d_1. Thus, we fitted the threshold voltage at each curing temperature with following equation:

$$V_{th} = \frac{B}{d_1} = B\sqrt{\frac{(1 - \mathrm{T}/\mathrm{T_c})^{\beta} \exp(\mathrm{E_b}/\mathrm{k_B T})}{T}}, \tag{9}$$

here B is a fitting parameter, while T_c and β maintain unchanged. As shown in Fig. 1, good agreement is obtained with B = 26.5 $V\sqrt{K}$. and E_b = 137.5 meV. The obtained activation energy is within 5% of that fitted with Eq. (8), which confirms the validity of our physical model between domain size and curing temperature. Since both operation voltage and response time are determined by the domain size, this physical model provides useful guidelines to optimize the domain size by controlling curing temperature.

When the curing temperature is further increased to 73°C, $V_{2\pi}$ drops to 22.8V as Fig. 3(a) shows, which is within the reach of LCoS. Figure 3(b) shows the measured decay time of a reflective PNLC cell whose initial biased voltage is 22.8V. Similar to measuring the free relaxation time, the biased voltage was removed instantaneously at t = 0. The measured phase decay time from 100% to 10% is 1.13ms, which is 2X faster than that previously reported [16].

#226549 - $15.00 USD Received 7 Nov 2014; revised 14 Jan 2015; accepted 15 Jan 2015; published 28 Jan 2015

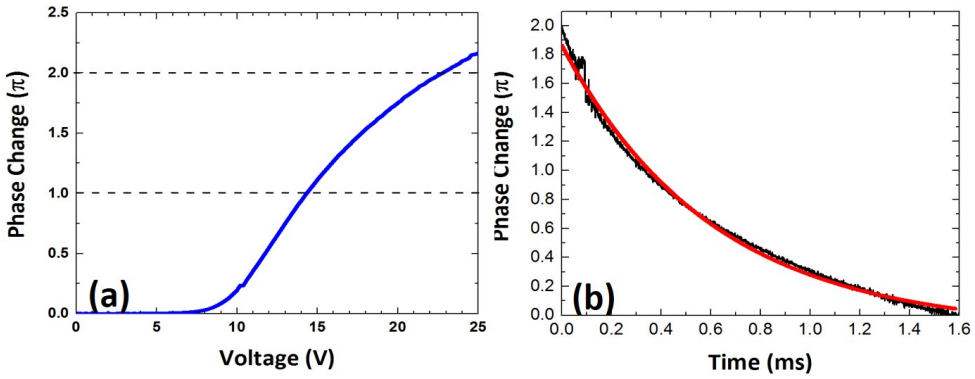

Fig. 3. (a) Voltage-dependent phase change at λ = 1.55μm for a PNLC cured at 73°C with $V_{2\pi}$ = 22.8V. (b) Measured phase decay time of the PNLC sample. Black line is experimental data and red line is fitting result with Eq. (4) and $\delta_o = 2\pi$.

Table 1. Physical properties and figure of merits of five LC hosts used in PNLCs.

LC mixtures	Δn (λ = 633nm)	$\Delta\varepsilon$	γ_1 (Pa·s)	FoM_1 ($\Delta\varepsilon\Delta n^2/\gamma_1$) $(Pa\cdot s)^{-1}$	FoM_2 ($\Delta\varepsilon/\gamma_1$) $(Pa\cdot s)^{-1}$
HTG135200 (HCCH)	0.21	86	1.20	3.16	71.67
JC-BP07N (JNC)	0.17	302	3.88	1.82	77.84
E44 (Merck)	0.24	16	0.33	2.79	48.48
BL038 (Merck)	0.25	16	0.56	1.79	28.57
BP1 (HCCH)	0.15	50	1.52	0.74	32.89

3. Figure of merit (*FoM*) of LC host

The overall performance of a PNLC device is governed by three key parameters: 1) 2π phase change, 2) low operation voltage, and 3) fast response time. The phase change requirement is determined by Eq. (1). The Δn employed in a PNLC device is slightly smaller than that of the LC host because the polymer network makes no contribution. The on-state voltage and response time are described by Eqs. (2) and (3), respectively. Therefore, besides the cell gap and domain size, the physical properties of LC host also play a key role in determining the overall performance of PNLC. As discussed above, the domain size can be controlled by the monomer concentration and curing temperature. If a certain phase change (say $\delta = 2\pi$) is required, then the cell gap should satisfy following simple condition:

$$d = \lambda / \Delta n. \tag{10}$$

By substituting Eq. (10) into Eq. (2), the correlation between $V_{2\pi}$ and Δn is found:

$$V_{2\pi} \sim \frac{\lambda}{\Delta n d_1}\sqrt{\frac{K_{11}}{\varepsilon_0 \Delta\varepsilon}}. \tag{11}$$

To balance the overall performance, response time needs to be considered as well [25]. To eliminate the effect of domain size, based on Eqs. (3) and (11), here we define a Figure of Merit (FoM_1) to evaluate the properties of LC host as:

$$FoM_1 = 1/(V_{2\pi}^2 \tau) \sim \Delta\varepsilon \Delta n^2 / \gamma_1. \tag{12}$$

Therefore, the FoM_1 is independent of the domain size and elastic constant (K_{11}). From Eq. (12), LC host with a large $\Delta\varepsilon$, Δn and small γ_1 is preferred for PNLC devices. If the cell gap is fixed, then we take the product of Eq. (3) and the square of Eq. (2) directly, and FoM_1 could be simplified to:

#226549 - $15.00 USD Received 7 Nov 2014; revised 14 Jan 2015; accepted 15 Jan 2015; published 28 Jan 2015

$$FoM_2 = 1/(V_{2\pi}^2 \tau) \sim \Delta\varepsilon / \gamma_1. \quad (13)$$

Table 1 lists several LC hosts we employed for making PNLC devices. HTG 135200 (HCCH, China) shows the highest FoM_1 among those LC mixtures due to its relatively high birefringence and dielectric anisotropy. However, if the cell gap is fixed, then JC-BP07N shows the best performance due to its extremely large $\Delta\varepsilon$. Thus, for $\lambda = 1.55\mu m$ and $d = 11.8\mu m$, JC-BP07N is a good host. When the curing temperature is increased to 73°C, the operation voltage is reduced to below 24V. However, JC-BP07 has a lower FoM_2 than HTG135200 because of its lower birefringence. From Eqs. (12) and (13), FoM_1 and FoM_2 are sensitive to the temperature because birefringence, rotational viscosity and dielectric anisotropy are also temperature dependent [11, 22, 26]:

$$\Delta n = \Delta n_0 (1 - \mathrm{T}/\mathrm{T_c})^{\beta}, \quad (14)$$

$$\gamma_1 \sim S \cdot \exp(E_b / k_B T), \quad (15)$$

$$\Delta\varepsilon = C \cdot S \exp(\mathrm{U}/k_B T), \quad (16)$$

where Δn_0 is the extrapolated birefringence at $T = 0K$, C is a fitting parameter, and U is a parameter related to the dipole moment. By combining these equations, the temperature dependency of FoM_1 is derived as:

$$FoM_1 = D \cdot \frac{(1 - \mathrm{T}/\mathrm{T_c})^{2\beta}}{\exp((\mathrm{E}_a - \mathrm{U})/\mathrm{k_B T})}, \quad (17)$$

here D is a fitting parameter. As shown in Fig. 4, dots stand for the measured data and red line for the fitting results with Eq. (17) for JC-BP07N. Good agreement is obtained with following fitting parameters: $D = 8.98 \times 10^6$, $U = 207.8$ meV, $E_a = 575.3$ meV, $\beta = 0.16$ and $T_c = 87$°C. β, E_a and U are obtained by fitting Eqs. (14), (15) and (16) respectively. Since the polymer network (i.e. domain size) and device structure are independent of operating temperature, the temperature dependent performance of PNLC is basically determined by the employed LC host only. At room temperature, the FoM_1 is ~4.79 $\mu m^2/s$ and it increases to 11.35 $\mu m^2/s$ at 60þC. As the temperature increases, viscosity decreases more quickly than birefringence and dielectric anisotropy initially, resulting in an increased FoM_1. As T approaches T_c, Δn decreases more quickly than γ_1, leading to a sharply declined FoM_1. On the other hand, the temperature dependent FoM_2 is expressed as:

$$FoM_2 \sim \exp((\mathrm{U} - E_a)/\mathrm{k_B T}). \quad (18)$$

FoM_2 increases as the temperature gets higher, because the fitting parameter U is usually smaller than the activation energy E_a for LC hosts [26]. Therefore, for a given PNLC an optimal operation temperature (T_{op}) exists which gives the maximum FoM_1. To derive the optimal temperature, we set $d(\mathrm{FoM})/\mathrm{dT} = 0$ and find that

$$T_{opt} = T_c - \frac{2\beta k_B T_c^2}{E_a - U}. \quad (19)$$

By substituting the fitting parameters of JC-BP07N, we found $T_{op} = 77.4$°C, or the optimal operation temperature is about 10°C lower than the clearing point. At T_{op}, FoM_1 has a peak value even though the operation voltage would increase due to the decreased $\Delta\varepsilon$. Therefore, the device can be operated at T_{op} if fast response time is the primary requirement.

#226549 - $15.00 USD Received 7 Nov 2014; revised 14 Jan 2015; accepted 15 Jan 2015; published 28 Jan 2015

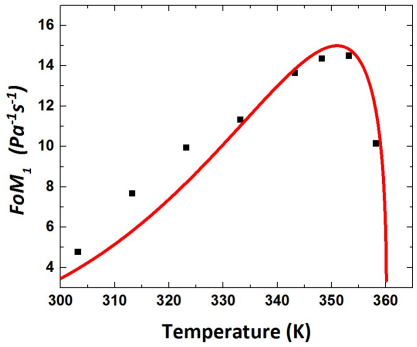

Fig. 4. Temperature dependent FoM_1 for JC-BP07N at λ = 633nm: dots stand for the measured data and red line for fitting curve with Eq. (17)

4. Conclusion

We have developed a physical model to correlate the curing temperature and domain size. The proposed equation fits very well with the experimental data, which also provides a good approach to optimize the curing temperature. Besides, we defined a *FoM* to compare the performance of LC hosts for PNLC devices. For a given LC host, there is an optimal temperature for achieving maximum *FoM*. Therefore, by increasing curing temperature to 73°C and employing a LC host with large $\Delta\varepsilon$, we have achieved $V_{2\pi}$ = 22.8V in reflective mode operating at infrared region (λ = 1.55μm).With keeping uniform phase profile, the response time is only half of previous reported. Such a low operation voltage will allow PNLC to be integrated in a high resolution LCoS for next-generation SLM applications.

Acknowledgment

The authors are indebted to AFOSR for the financial supports under contract No. FA9550-14-1-0279.

#226549 - $15.00 USD Received 7 Nov 2014; revised 14 Jan 2015; accepted 15 Jan 2015; published 28 Jan 2015